

# Electronic Supplementary Information

## Intramolecular and interfacial dynamics of triarylamine-based hole transport materials

*Johannes R. Klein, Mirko Scholz, Kawon Oum\* and Thomas Lenzer*

Universität Siegen, Physikalische Chemie, Adolf-Reichwein-Str. 2, 57076 Siegen, Germany

E-mail: [oum@chemie.uni-siegen.de](mailto:oum@chemie.uni-siegen.de)

### Table of Contents

1.	Results of the global kinetic analysis for X60 in THF.....	2
2.	Kinetic fits for X60 on mesoporous TiO <sub>2</sub> .....	6
3.	Coherent oscillation for PTAA in THF.....	7
4.	Kinetic fits for PTAA in THF and on mesoporous TiO <sub>2</sub> .....	8
5.	Transient absorption spectra of HTM-MAPI-TiO <sub>2</sub> thin films.....	10
6.	Reference .....	13

# 1. Results of the global kinetic analysis for X60 in THF

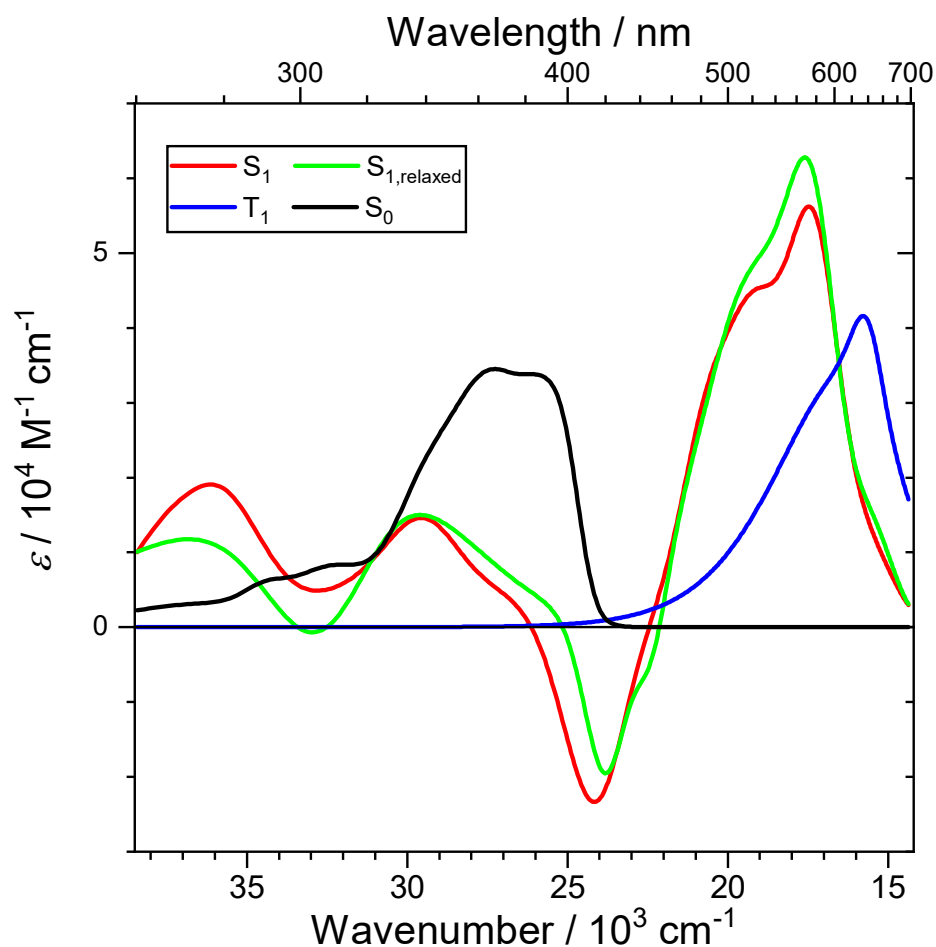


**Figure S1.** Species-associated spectra (SAS) for X60 in THF obtained from the global kinetic analysis. Absolute absorption coefficients of the species are referenced to the peak of the  $S_0$  absorption spectrum. The latter was estimated as  $34500 \text{ M}^{-1} \text{ cm}^{-1}$  which is 50% of the value provided by Bach for *spiro*-OMeTAD in chlorobenzene ( $69000 \text{ M}^{-1} \text{ cm}^{-1}$ ),<sup>1</sup> because the latter HTM has two fluorene units instead of one in the case of X60. We note that the  $S_0$  spectrum of X60, which was used in the global analysis, only contains the “bleached part” of the experimental steady-state absorption spectrum (see Fig. 2(A) and the top panel of Fig. 4 of the main manuscript), but not the intense peak at 300 nm which arises from the “isolated” triarylamine units (Fig. 1(B), main manuscript). The latter ones are not excited by the 400 nm pump pulse.

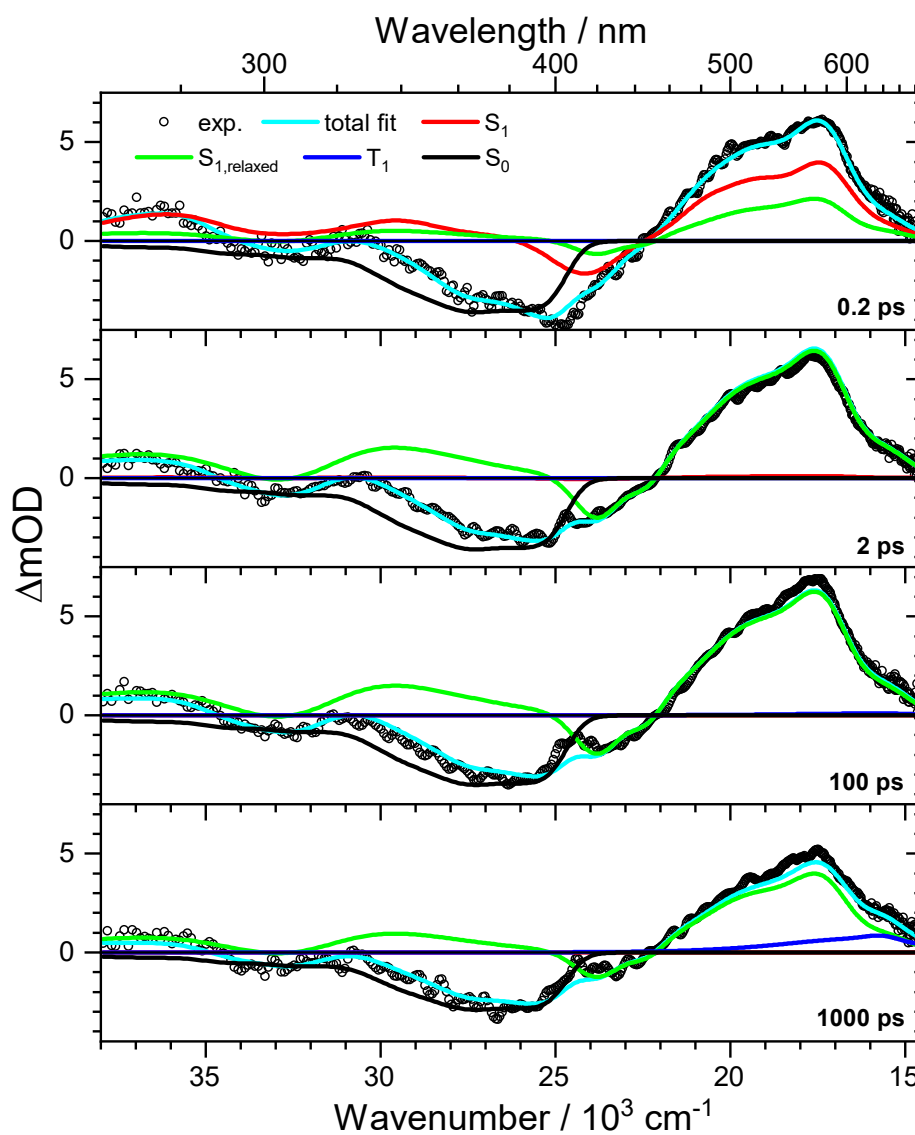


**Figure S2.** Contributions of the different electronic species to the PSCP spectra of X60 in THF obtained from the global kinetic analysis. Results are shown for the delay times 0.2, 2, 100 and 1000 ps.

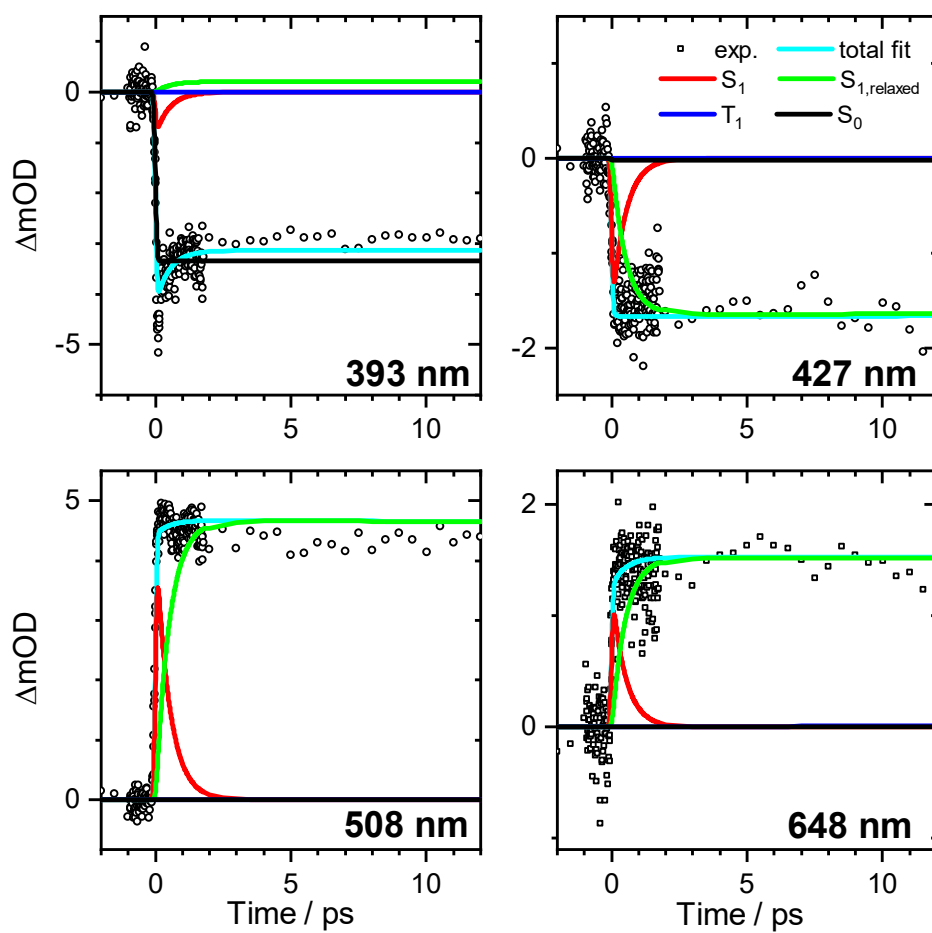


**Figure S3.** Kinetic fits including contributions of the different electronic species for X60 in THF obtained from the global kinetic analysis. Representative results are shown for the probe wavelengths 393, 427, 508 and 648 nm at early times up to 12 ps.

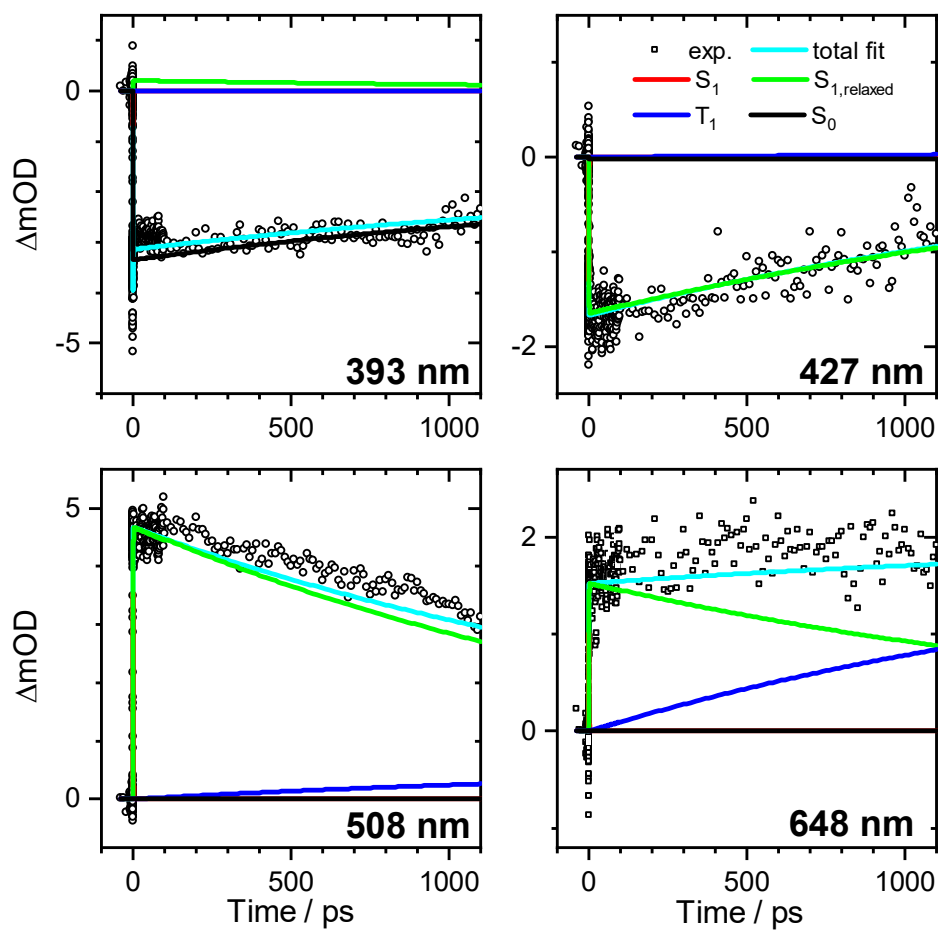


**Figure S4.** Same as in Fig. S3, but for delay times up to 1100 ps.

## 2. Kinetic fits for X60 on mesoporous TiO<sub>2</sub>

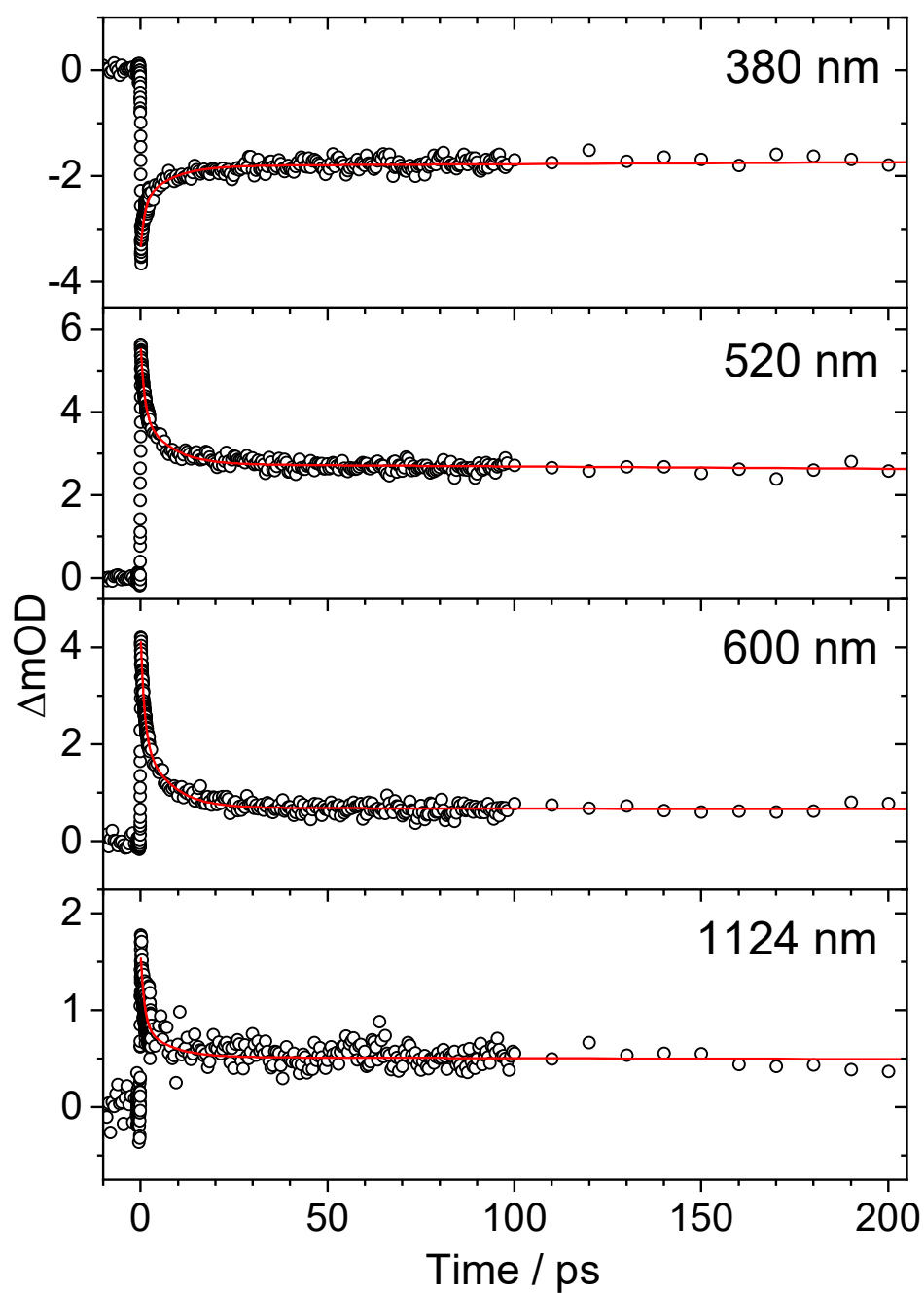


**Figure S5.** Kinetic traces for X60 on mesoporous TiO<sub>2</sub> at selected wavelengths including triexponential fits with the time constants  $\tau_1 = 1.0$ ,  $\tau_2 = 7.1$  and  $\tau_3 = 5000$  ps (see Table 1, main manuscript).

### 3. Coherent oscillation for PTAA in THF

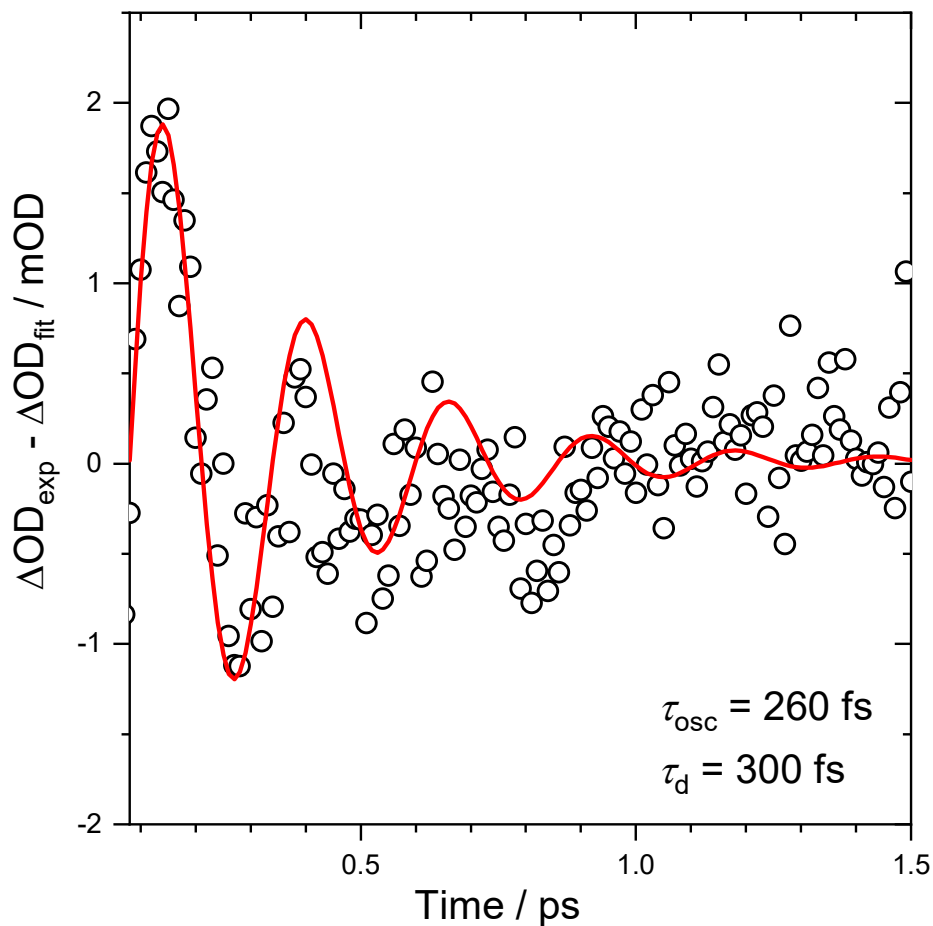


**Figure S6.** Coherent oscillation in the PSCP spectra for PTAA in THF at the probe wavelength 400 nm. After subtraction of a decay function with  $\tau_1 = 0.2$  and  $\tau_2 = 3.3$  ps (see Table 2, main manuscript) the decaying oscillation was fitted by a damped sine function (red line) providing the oscillation period  $\tau_{\text{osc}} = 260$  fs (corresponding to a vibration of  $128 \text{ cm}^{-1}$ ) and the time constant  $\tau_d = 300$  fs for the decoherence process.

#### 4. Kinetic fits for PTAA in THF and on mesoporous TiO<sub>2</sub>

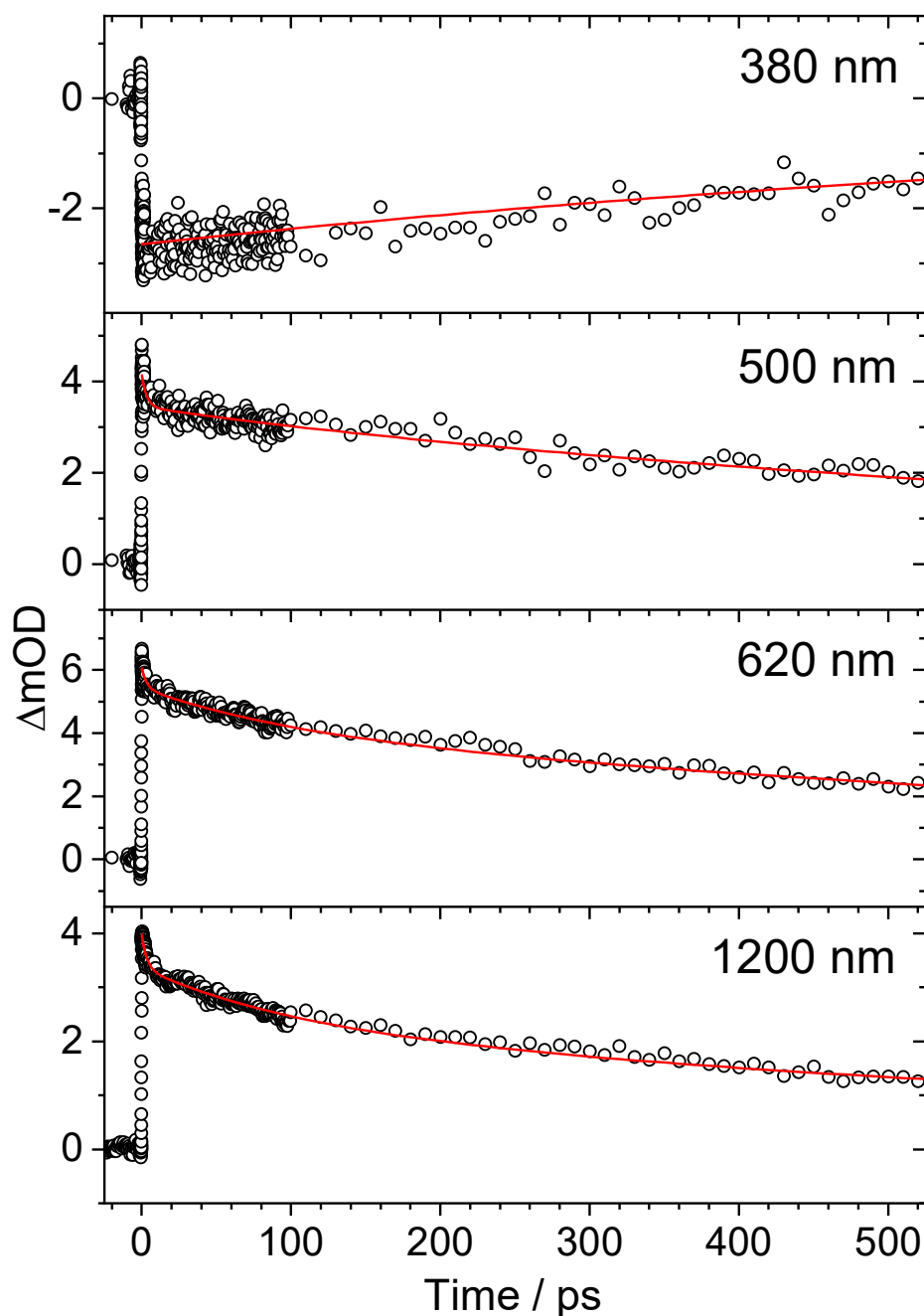


**Figure S7.** Kinetic traces for PTAA in THF at selected wavelengths including fits. Note that the fits for the three wavelengths in the ESA bands contain the time constants  $\tau_2 = 3.3$ ,  $\tau_3 = 96$  and  $\tau_4 = 900$  ps (see also Table 2, main manuscript), where  $\tau_2$  and  $\tau_3$  reflect dynamics of the singlet excitons and  $\tau_4$  describes the recombination of the singlet excitons repopulating  $S_0$ . In contrast, the kinetics in the ground state bleach region (380 nm) only contains the slow time constant  $\tau_4$ , *i.e.* the recombination of singlet excitons.



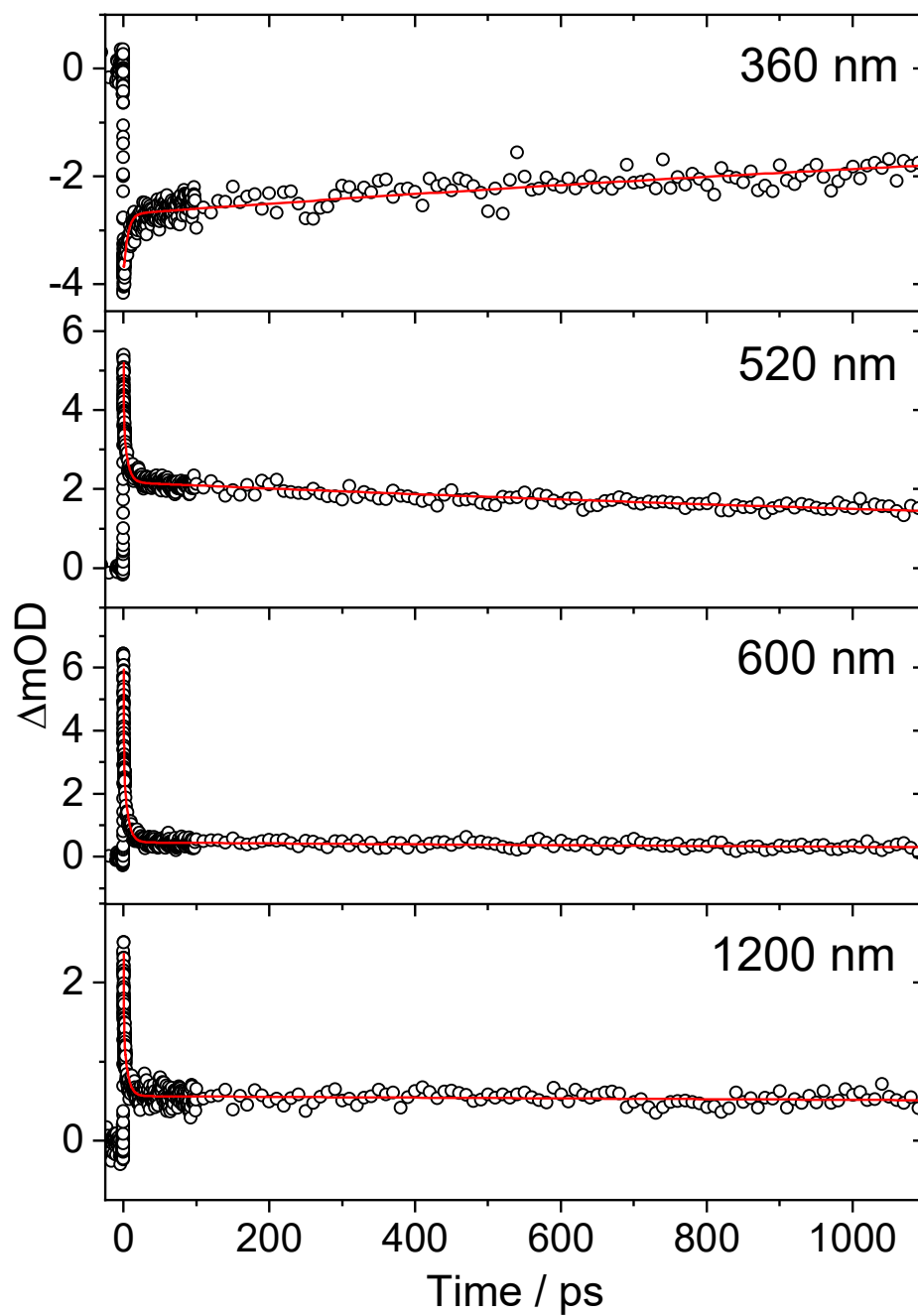


**Figure S8.** Kinetic traces for PTAA on mesoporous  $TiO_2$  at selected wavelengths including fit lines. See also Table 2 in the main manuscript.

## 5. Transient absorption spectra of HTM-MAPI-TiO<sub>2</sub> thin films

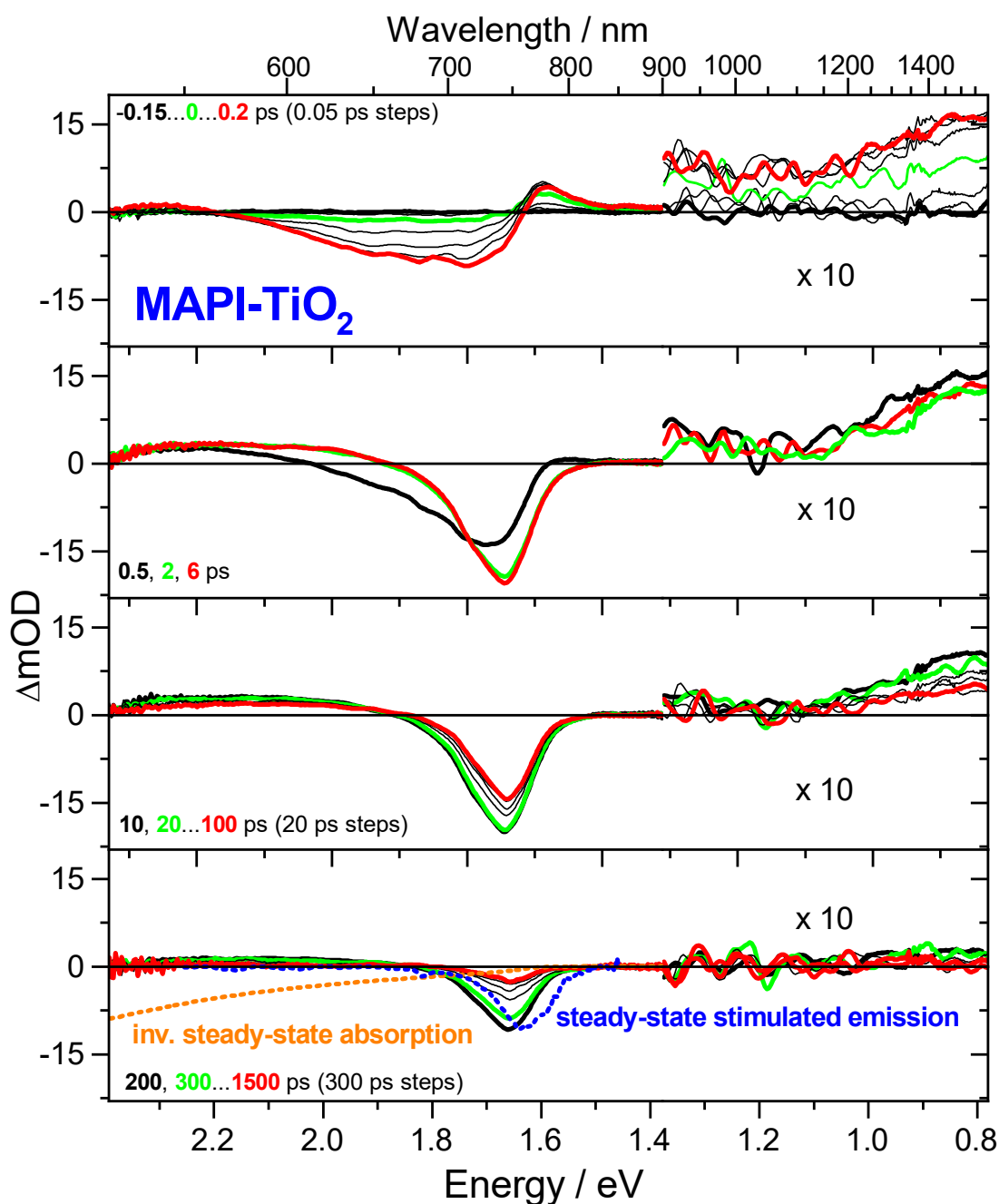


**Figure S9.** Broadband PSCP Vis-NIR transient absorption spectra for MAPI-TiO<sub>2</sub>. Different time ranges of interest are indicated in the individual panels. Note that all spectra in the NIR range have been magnified by a factor of 10 for the sake of clarity. The dashed orange and blue lines in the bottom panel represent the scaled inverted steady-state absorption and stimulated emission spectra. Pump wavelength: 505 nm.

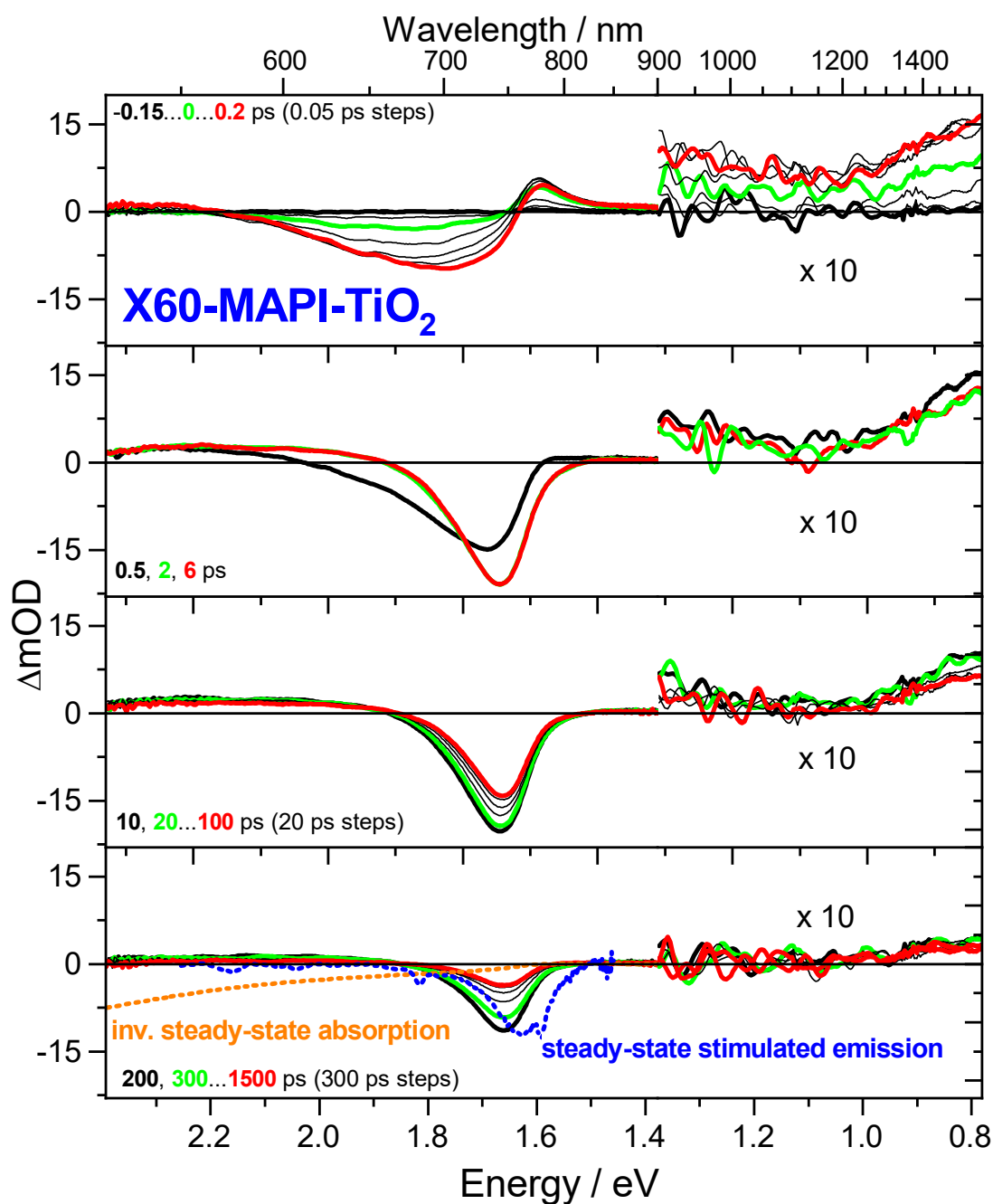


**Figure S10.** Broadband PSCP Vis-NIR transient absorption spectra for X60-MAPI-TiO<sub>2</sub>. Different time ranges of interest are indicated in the individual panels. Note that all spectra in the NIR range have been magnified by a factor of 10 for the sake of clarity. The dashed orange and blue lines in the bottom panel represent the scaled inverted steady-state absorption and stimulated emission spectra. Pump wavelength: 505 nm.

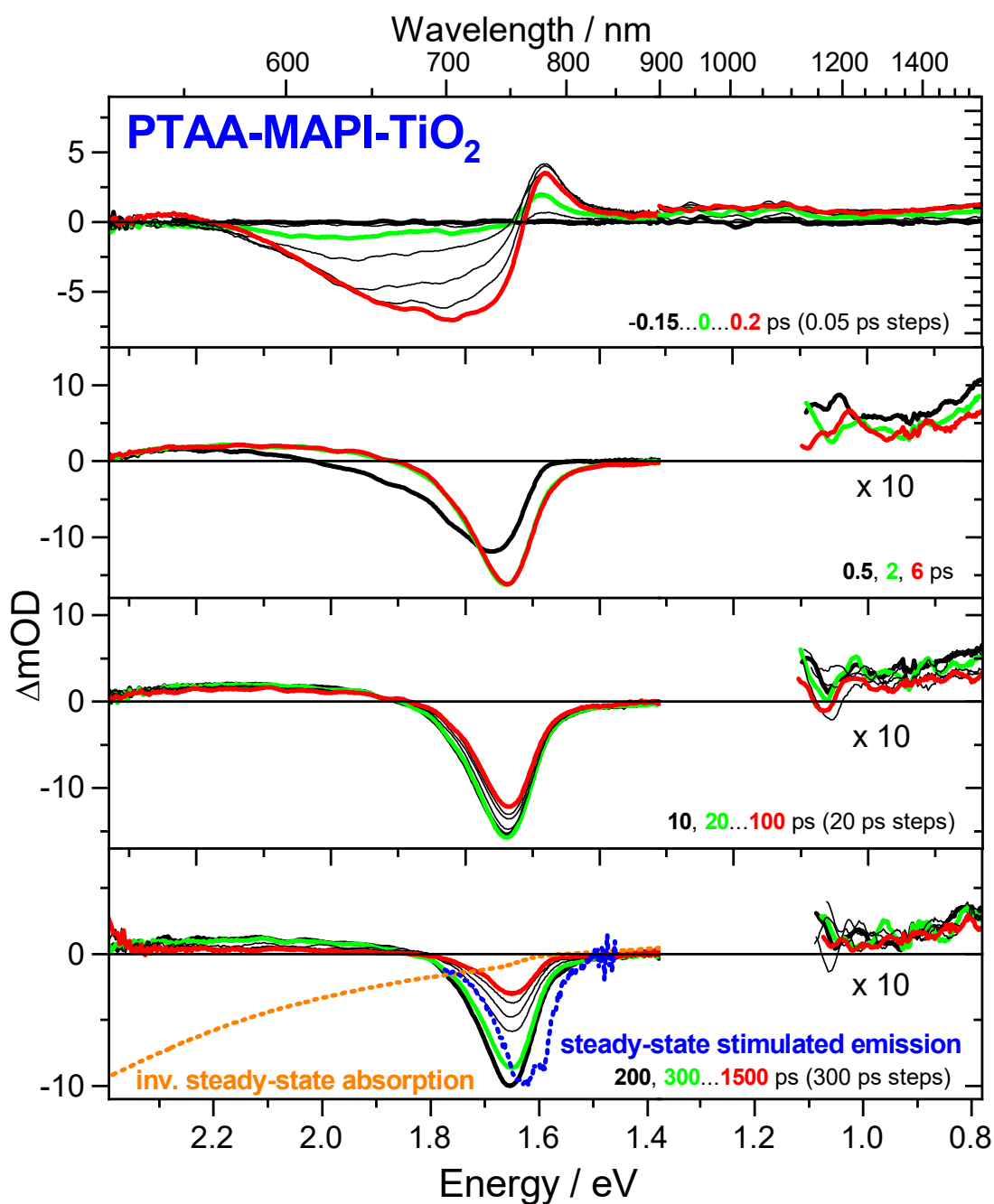


**Figure S11.** Broadband PSCP Vis-NIR transient absorption spectra for PTAA-MAPI-TiO<sub>2</sub>. Different time ranges of interest are indicated in the individual panels. Note that the NIR spectra in the second to fourth panel have been magnified by a factor of 10 for the sake of clarity. The dashed orange and blue lines in the bottom panel represent the scaled inverted steady-state absorption and stimulated emission spectra. Pump wavelength: 505 nm.

## **6. Reference**

1. U. Bach, Solid-state dye-sensitized mesoporous  $\text{TiO}_2$  solar cells, Ph. D. thesis, École Polytechnique Fédérale de Lausanne, 2000.